

# Effective Field Theory and Finite Density Systems

RICHARD J. FURNSTAHL

*Department of Physics, Ohio State University; email: furnstahl.1@osu.edu*

GAUTAM RUPAK AND THOMAS SCHÄFER

*Department of Physics, North Carolina State University; email: grupak@gmail.com, tmschaef@ncsu.edu*

**Key Words** nuclear matter, many-body physics, chiral symmetry

**Abstract** This review gives an overview of effective field theory (EFT) as applied at finite density, with a focus on nuclear many-body systems. Uniform systems with short-range interactions illustrate the ingredients and virtues of many-body EFT and then the varied frontiers of EFT for finite nuclei and nuclear matter are surveyed.

## CONTENTS

INTRODUCTION . . . . .	1
EFT FOR UNIFORM SYSTEMS . . . . .	4
<i>Prototype Many-Body EFT</i> . . . . .	4
<i>EFT Near the Fermi Surface</i> . . . . .	7
<i>Unnatural Scattering Length</i> . . . . .	9
EFT FOR FINITE NUCLEI AND NUCLEAR MATTER . . . . .	12
<i>Pion Physics From Chiral EFT</i> . . . . .	12
<i>Wave Function Methods</i> . . . . .	15
<i>EFT on the Lattice</i> . . . . .	17
<i>Perturbative EFT for Nuclear Matter</i> . . . . .	19
<i>Density Functional Theory as an EFT</i> . . . . .	21
SUMMARY AND OUTLOOK . . . . .	23

## 1 INTRODUCTION

Calculating the properties of atomic nuclei and nuclear matter starting from microscopic internucleon forces is one of the oldest unsolved challenges of nuclear physics. Renewed interest in this problem is fueled by experiments at rare isotope facilities, which open the door to new domains of unstable nuclides that are not all accessible in the lab, and by descriptions of astrophysical

phenomena such as supernovae and neutron stars, which require controlled extrapolations of the equation of state of nuclear matter in density, temperature, and proton fraction [1]. But despite decades of work and technological advances, there remain severe computational barriers and only limited control of uncertainties in conventional nuclear many-body calculations of all but the lightest nuclei. The difficulties are exacerbated by the need to supplement accurate phenomenological two-nucleon potentials with poorly understood many-body forces to achieve a quantitative (and in many cases qualitative) description of nuclei. Finally, conventional approaches are at best loosely connected to quantum chromodynamics (QCD), the underlying theory of the strong interaction.

Effective field theory (EFT) provides new tools to address these challenges. The goals of EFT applied to finite density nuclear systems are to put nuclear many-body physics on a firm foundation so that it can be *i)* systematically improved with associated theoretical error bars, *ii)* extended reliably to regimes where there is limited or no data, and *iii)* connected to QCD as well as to few-body experiments. Our modest aim for this review is to give a flavor for how EFT can accomplish these goals in many-body systems and to survey the frontiers of EFT-based calculations of many-body nuclei and nuclear matter.

Any EFT builds on a basic physics principle that underlies *every* low-energy effective model or theory. A high-energy, short-wavelength probe sees details down to scales comparable to the wavelength. Thus, electron scattering at sufficiently high energy reveals the quark substructure of protons and neutrons in a nucleus. But at lower energies, details are not resolved, and one can replace short-distance structure with something simpler, as in a multipole expansion of a complicated charge or current distribution. This means it is not necessary to calculate with full QCD to do accurate strong interaction physics at low energies; we can replace quarks and gluons by neutrons and protons (and maybe pions and ...). Effective field theory provides a systematic, model-independent way to carry out this program starting with a local Lagrangian framework.

An EFT is formulated by specifying appropriate low-energy degrees of freedom and then constructing the Lagrangian as a complete set of terms that embody the symmetries of the underlying theory. (Note: the general Lagrangian will typically be *overcomplete*, but redundant terms can be removed by redefining the fields appropriately.) There is not a unique EFT for nuclear physics. In different applications the relevant degrees of freedom might be neutrons and protons only, or neutrons, protons, and pions, or neutrons, protons, pions, and  $\Delta$ 's or quasi-nucleons. The form of the EFT can be chosen to readily expose universal behavior, such as features dilute neutron matter has in common with phenomena seen in cold atom experiments.

In applying an EFT Lagrangian, one must confront in a controlled way the impact of excluded short-distance physics. Quantum mechanics implies that sensitivity to short-distance physics is *always* present in a low-energy theory, but it is made manifest in an EFT through dependence on a cutoff or other regulator instead of being hidden in phenomenological form factors. Removing this dependence necessitates a well-defined regularization and renormalization scheme as part of the EFT specification. This necessity becomes a virtue as residual regulator dependence can be used to assess truncation errors and many-body approximations. Furthermore, the freedom in how to regulate coupled with the freedom to make unitary transformations can be exploited by renormalization group methods to greatly simplify few- and many-body nuclear calculations.

For an EFT calculation to be improvable order-by-order, one needs a scheme to organize the infinity of possible terms in the Lagrangian based on an expansion parameter (or parameters).

Such a scheme is called a power counting. Power counting tells us what terms (or Feynman diagrams) to include at each order and lets us estimate the theoretical truncation error. The radius of convergence associated with the expansion means that the EFT predicts its own downfall, in contrast to phenomenological models. EFT expansion parameters most commonly arise as a ratio of disparate physical scales rather than as a small coupling constant (*e.g.*, as in Coulomb systems); a many-body example is the ratio of the range of the interaction to the interparticle spacing in a dilute system. The power counting for this example is particularly simple when the scattering length is roughly the same size as the interaction range (called “natural”) but changes dramatically if the scattering length is much larger (called “unnatural”). We will explore both situations below.

Chiral effective field theory is a faithful low-energy realization of QCD whose power counting takes advantage of the spontaneously broken chiral symmetry that gives rise to the almost massless (on hadronic scales) pion. It has the potential to bridge the gap between QCD and nuclei, letting us explore how nuclear properties depend on QCD parameters (*e.g.*, how would the binding energies of nuclei change if the light quark masses were different or if the QCD scale parameter were time dependent?) and opening a connection to *ab initio* QCD lattice calculations. Chiral EFT power counting explains the empirical hierarchy of many-body forces in nuclear physics, fixes their natural sizes, and gives an organizing principle for their construction. Other compelling features are the systematic inclusion of relativistic corrections and prescriptions for consistent currents needed to predict experimental observables.

It is probably evident that a comprehensive treatment of EFT and finite density nuclear systems would require several extended reviews covering EFT in general, EFT applied to internucleon interactions, and field theory at finite density. Fortunately there are recent articles in this journal to provide much of the background for the interested reader; these include an introduction to effective field theory by Burgess [2], an overview of chiral perturbation theory by Bernard and Meißner [3], and a review of EFT for few-nucleon systems by Bedaque and van Kolck [4] (see also refs. [5, 6]). We will focus here on illustrating how the basic principles of EFT can be realized at finite density and on surveying various applications to nuclear matter and finite nuclei. Our treatment will be schematic in most cases and we will refer the reader to the literature for details.

In Section 2, we consider uniform systems with short-range interactions. The dilute Fermi gas with repulsive interactions serves as a prototype for EFT at finite density while new features and techniques arise when we study physics near the Fermi surface. Many-body systems with unnatural scattering lengths, which manifest various forms of universal physics, are attacked by a variety of nonperturbative EFT techniques. Actual applications of EFT to nuclear many-body systems are in their infancy and there are multiple frontiers; a range of examples are described in Section 3. These start with the use of chiral EFT interactions as input to conventional many-body wave function methods applicable to light nuclei and a pioneering attempt to apply EFT to the methods themselves. Lattice calculations provide a complementary nonperturbative approach. Perturbative chiral EFT calculations for nuclei may be possible, however, if the power counting differs at nuclear densities. This may be justified by renormalization group transformations that soften the chiral interactions. Finally, density functional theory (DFT), which is computationally tractable for all nuclides, is naturally cast in EFT form using effective actions. We conclude in Section 4 with a summary of the current status of EFT for nuclear systems, on-going developments, important open questions, and pointers to omitted topics.

## 2 EFT FOR UNIFORM SYSTEMS

In this section, we illustrate the ideas of EFT at finite density for uniform systems with short-range interactions.

### 2.1 Prototype Many-Body EFT

We start with perhaps the simplest possible application, a dilute Fermi system with repulsive, spin-independent interactions of range  $R$ . A concrete example would be “hard sphere” repulsion at radius  $R$ , which can be viewed as a caricature of the short-range part of the nuclear force. In perturbation theory all matrix elements of this potential are infinite; while a more realistic potential would not be so extreme, textbook treatments of this many-body problem all start with nonperturbative summations and then expansions at low-density [7]. In contrast, the EFT approach directly exploits the essential physics that the “hard core” is not resolved at low momentum.

With either approach, the end result for free space, two-particle scattering at low energies ( $\lambda = 2\pi/k \gg 1/R$ ) is the effective range expansion; *e.g.*, the  $s$ -wave phase shift  $\delta_0(k)$  satisfies:

$$k \cot \delta_0(k) \xrightarrow{k \rightarrow 0} -\frac{1}{a_0} + \frac{1}{2}r_0 k^2 + \dots \quad (1)$$

where  $a_0$  is the scattering length and  $r_0$  is the effective range. The system is said to have a “natural” scattering length if it is the same order as the range of the interaction (*e.g.*,  $a_0 = R$  and  $r_0 = 2R/3$  for hard spheres). In a later section we consider the case of unnatural scattering length, with  $a_0 \gg R$ , which is relevant for dilute neutron matter and cold atom systems. For a natural system, the dilute expansion of the energy density for a uniform system starts as ( $s$ -wave only here)

$$\mathcal{E} = \rho \frac{k_F^2}{2M} \left[ \frac{3}{5} + (\nu - 1) \left\{ \frac{2}{3\pi} (k_F a_0) + \frac{4}{35\pi^2} (11 - 2 \ln 2) (k_F a_0)^2 + \frac{1}{10\pi} (k_F r_0) (k_F a_0)^2 \right\} + \dots \right], \quad (2)$$

where  $k_F$  is the Fermi momentum,  $\nu$  is the spin degeneracy, and  $\rho = \nu k_F^3 / 6\pi^2$ . This result arises very cleanly from an EFT treatment [8].

Consider the ingredients for any effective field theory along with the specifics for this example:

1. *Use the most general  $\mathcal{L}$  with low-energy degrees-of-freedom consistent with global and local symmetries of the underlying theory.* Here we have nucleons only with Galilean invariance and discrete symmetries. A general interaction is then a sum of delta functions and derivatives of delta functions with two-body (four fields), three-body (six-fields), and so on, so  $\mathcal{L}_{\text{eff}}$  is

$$\mathcal{L}_{\text{eff}} = \psi^\dagger \left[ i \frac{\partial}{\partial t} + \frac{\nabla^2}{2M} \right] \psi - \frac{C_0}{2} (\psi^\dagger \psi)^2 + \frac{C_2}{16} [(\psi \psi)^\dagger (\psi \overleftrightarrow{\nabla}^2 \psi) + \text{h.c.}] - \frac{D_0}{6} (\psi^\dagger \psi)^3 + \dots, \quad (3)$$

where  $\dots$  indicates terms with more derivatives and more fields. (We have eliminated higher-order time derivatives using the equations of motion [8].) The  $\psi$ 's have  $\nu$  components and spin-indices are implicit (and contracted between  $\psi^\dagger$  and  $\psi$ ).

2. *Declare a regularization and renormalization scheme.* One choice is to smear out the delta functions (*e.g.*, as gaussians in momentum space) to introduce a cutoff; renormalization would remove cutoff dependence. However, for a natural  $a_0$ , using dimensional regularization and minimal subtraction (rather than a cutoff) is particularly convenient and efficient.

3. *Establish a well-defined power counting*, which means identifying small expansion parameters, typically using a ratio of scales. In free space  $k/\Lambda$  with  $\Lambda \sim 1/R$  is the clear choice, and then  $k_F/\Lambda$  is the corresponding parameter in the medium. Dimensional analysis, with some additional insight to give us the  $4\pi$ 's, implies ( $2i$  denotes the number of gradients)

$$C_{2i} \sim \frac{4\pi}{M} R^{2i+1}, \quad D_{2i} \sim \frac{4\pi}{M} R^{2i+4}, \quad (4)$$

which will enable us to make quantitative power-counting estimates.

Feynman diagrams and rules for the EFT follow from conventional formalism for free-space and many-body perturbation theory (*e.g.*, see [7, 9]).

The constants  $C_{2i}$  are determined by matching to the free-space scattering amplitude  $f_0(k)$  in perturbation theory,

$$f_0(k) = \frac{4\pi}{M} \left( a_0 - i a_0^2 k - a_0^3 k^2 + a_0^2 r_0 k^2 + \dots \right). \quad (5)$$

The leading potential  $V_{\text{EFT}}^{(0)}(\mathbf{x}) = C_0 \delta(\mathbf{x})$  or  $\langle \mathbf{k} | V_{\text{eff}}^{(0)} | \mathbf{k}' \rangle = C_0$ , where  $\mathbf{k}, \mathbf{k}'$  are relative momenta. Matching to  $f_0(k)$  fixes  $C_0 = 4\pi a_0/M$  at leading order, which then determines the leading finite density contribution (Hartree-Fock) in Eq. (2) after sums over the Fermi sea:

$$\text{Diagram} \rightarrow C_0 \implies \text{Diagram} \rightarrow \mathcal{E}_{\text{LO}} = \frac{C_0}{2} \nu(\nu-1) \left( \sum_{\mathbf{k}}^{k_F} 1 \right)^2 \propto a_0 k_F^6. \quad (6)$$

Similar matching yields  $C_2$  in terms of  $a_0$  and  $r_0$  and the corresponding Hartree-Fock contribution for the effective range.

At the next order is  $\langle \mathbf{k} | V_{\text{eff}}^{(0)} G_0 V_{\text{eff}}^{(0)} | \mathbf{k}' \rangle$ , which includes a linearly divergent loop integral:

$$\text{Diagram} \rightarrow C_0 M \int^{\Lambda_c} \frac{d^3 q}{(2\pi)^3} \frac{1}{k^2 - q^2 + i\epsilon} C_0 = C_0^2 M \left( \frac{\Lambda_c}{2\pi^2} - \frac{ik}{4\pi} + \mathcal{O}\left(\frac{k^2}{\Lambda_c}\right) \right). \quad (7)$$

We can redefine (“renormalize”)  $C_0$  to absorb the linear dependence on the cutoff  $\Lambda_c$ , but we’ll have higher powers of  $k$  from every diagram. A more efficient scheme is dimensional regularization with minimal subtraction (DR/MS), which implies only one power of  $k$  survives:

$$\int \frac{d^D q}{(2\pi)^3} \frac{1}{k^2 - q^2 + i\epsilon} \xrightarrow{D \rightarrow 3} -\frac{ik}{4\pi}. \quad (8)$$

Then we get the second term in Eq. (5) automatically with no change in  $C_0$ . At higher orders there is exactly one power of  $k$  per diagram and *natural* coefficients [*i.e.*, consistent with Eq. (4)], so we can estimate truncation errors from simple dimensional analysis.

The contribution to the energy density has two terms, one of which vanishes identically. In the other, we get a linear divergence again,

$$\text{Diagram} \implies \text{Diagram} \rightarrow \mathcal{E}_{\text{NLO}} \propto \int_{k_F}^{\infty} \frac{d^3 q}{(2\pi)^3} \frac{C_0^2}{k^2 - q^2}, \quad (9)$$

but the *same* renormalization fixes it,

$$\int_{k_F}^{\infty} \frac{1}{k^2 - q^2} = \int_0^{\infty} \frac{1}{k^2 - q^2} - \int_0^{k_F} \frac{1}{k^2 - q^2} \xrightarrow{D \rightarrow 3} -\int_0^{k_F} \frac{1}{k^2 - q^2}, \quad (10)$$

and particles become holes through the renormalization. Pauli blocking doesn't change the free-space ultraviolet (short-distance) renormalization, since the density is a long-distance effect; after fixing free space, the in-medium renormalization is determined. We find  $\mathcal{E}_{\text{NLO}} \propto a_0^2 k_F^7$ .

The diagrammatic power counting with DR/MS is very simple, with each loop adding a power of  $k$  in free-space. At finite density, a diagram with  $V_{2i}^n$   $n$ -body vertices and  $2i$  gradients scales as  $(k_F)^\beta$  with

$$\beta = 5 + \sum_{n=2}^{\infty} \sum_{i=0}^{\infty} (3n + 2i - 5) V_{2i}^n. \quad (11)$$

This reproduces, for example, the leading order [ $\beta = 5 + (3 \cdot 2 + 2 \cdot 0 - 5) \cdot 1 = 6$ ] and next-to-leading order [ $\beta = 5 + (3 \cdot 2 + 2 \cdot 0 - 5) \cdot 2 = 7$ ] dependencies. The power counting is exceptionally clean, with a separation of vertex factors  $\propto a_0, r_0, \dots$  and a dimensionless geometric integral times  $k_F^\beta$ , with each diagram contributing to exactly one order in the expansion. There is a systematic hierarchy, since adding derivatives or higher-body interactions increases the power of  $k_F$ . The ratio of successive terms is  $\sim k_F R$  [*e.g.*, in Eq. (2)], so we can estimate excluded contributions.

The energy density (2) *looks* like a power series in  $k_F$ , but at higher order there are *logarithmic* divergences from 3-3 scattering, which indicate new sensitivity to short-distance behavior. A cutoff  $\Lambda_c$  serves as a resolution scale; as we increase  $\Lambda_c$ , we see more of the short-distance details. Observables (such as scattering amplitudes) must not vary with  $\Lambda_c$ , so changes must be absorbed in a coupling. But it can't be a coupling from 2-2 scattering, because we already took care of all the divergences there. We instead must use the point-like three-body force, whose coupling  $D_0(\Lambda_c)$  can absorb the dependence on  $\Lambda_c$  [10]. The diagrams are  $\propto (C_0)^4 \ln(k/\Lambda_c)$ , which means

$$\frac{d}{d\Lambda_c} \left[ \text{diagram 1} + \text{diagram 2} + \text{diagram 3} \right] = 0 \implies D_0(\Lambda_c) \propto (C_0)^4 \ln(a_0 \Lambda_c) \quad (12)$$

fixes the coefficient  $D_0(\Lambda_c)$ . Dimensional regularization is similar [8]. In turn this implies for the energy density,

$$\mathcal{O}(k_F^9 \ln(k_F)) : \text{diagram 1} + \text{diagram 2} + \dots \propto (\nu - 2)(\nu - 1) k_F^5 (k_F a_0)^4 \ln(k_F a_0) \quad (13)$$

without actually carrying out the calculation! Similar analyses can identify the higher logarithmic terms in the expansion of the energy density [10, 8]. This is an example of the inevitability of many-body forces in low-energy theories: when the resolution or degrees of freedom are changed, we will have many-body forces. Thus the question is not whether such forces are present, but how large they are. For nuclear physics, their natural size implies they cannot be neglected.

This brief tour of the EFT for a natural dilute Fermi gas included features common to many other applications. Even if we knew that the underlying physics was a hard-sphere potential, the EFT was easier to calculate than conventional approaches [7]. Further, the EFT directly reveals the universal nature of the many-body counterpart to the effective range expansion, which applies to any short-range repulsive potential. Of course, this example is very simple; there are many ways to generalize. Some are immediate: *e.g.*, we can account for short-range spin-dependent interactions by adding terms such as  $C_0^\sigma (\psi^\dagger \boldsymbol{\sigma} \psi) \cdot (\psi^\dagger \boldsymbol{\sigma} \psi)$ . If we consider unnatural scattering, however, then we must revisit the power counting and consider alternative expansion parameters since  $k_F a_0$  is no longer small. But first we turn from EFT for bulk properties to EFT near the Fermi surface.

## 2.2 EFT Near the Fermi Surface

The theory described in the last section is completely perturbative. At any order in the  $k_F R$  expansion only a finite number of diagrams has to be computed. There are two ways in which this expansion can fail. One possibility is that one of the effective range parameters (typically, the scattering length) is anomalously large, so that a certain class of diagrams has to be summed to all orders. We will study this problem in Section 2.3. A second possibility is that the density (and the Fermi momentum) is too large and  $k_F R$  ceases to be a useful expansion parameter. In this case it is possible to construct a different kind of effective field theory by focusing on quasi-particles in the vicinity of the Fermi surface, and using  $|k - k_F|/\Lambda$  as an expansion parameter. This effective theory is known as Landau Fermi liquid theory [11,12]. The Landau theory does not account for all properties of the many-body system, but it does describe phenomena that are sensitive to physics near the Fermi surface such as collective modes, pairing, transport properties, *etc.*

Fermi liquid theory was originally developed by Landau using intuitive arguments. These arguments were later confirmed by Abrikosov and others using diagrammatic many-body perturbation theory [13]. The modern view of Fermi liquid theory as an effective field theory was advocated by Shankar, Polchinski, and others [14,15]. Consider the effective action of non-interacting, nonrelativistic Fermions near a Fermi surface

$$S = \int dt \int \frac{d^3 p}{(2\pi)^3} \psi^\dagger(p) \left( i \frac{\partial}{\partial t} - v_F l_p \right) \psi(p) . \quad (14)$$

Here we have decomposed the momenta as  $\mathbf{p} = \mathbf{k} + \mathbf{l}_p$ , where  $\mathbf{k}$  is on the Fermi surface,  $|\mathbf{k}| = k_F$ , and  $\mathbf{l}_p$  is orthogonal to the Fermi surface. The Fermi velocity is defined as  $v_F = \partial E_p / \partial p$ , where  $E_p$  is the quasiparticle energy. The power counting can be established by studying the behavior of operators under transformations  $l_p \rightarrow s l_p$  that scale the momenta towards the Fermi surface. Writing  $E_p = E_F + v_F l_p + \mathcal{O}(l_p^2)$  we see that as  $s \rightarrow 0$  only the Fermi velocity survives, so the detailed form of the dispersion relation is irrelevant. Using  $d^3 p = k_F^2 (dl_p)(d\Omega)$  we observe that  $d^3 p \sim s$ ,  $dt \sim s^{-1}$ , and  $\psi \sim s^{-1/2}$  and  $S$  in (14) is  $\mathcal{O}(s^0)$ .

We can now study the importance of interactions between fermions near the Fermi surface. The most general four-fermion interaction is of the form

$$S_{4f} = \frac{1}{4} \int dt \left[ \prod_{i=1}^4 \int \frac{d^3 p_i}{(2\pi)^3} \right] \psi^\dagger(\mathbf{p}_4) \psi^\dagger(\mathbf{p}_3) \psi(\mathbf{p}_2) \psi(\mathbf{p}_1) \delta^3(\mathbf{p}_{\text{tot}}) U(\mathbf{p}_4, \mathbf{p}_3, \mathbf{p}_2, \mathbf{p}_1) , \quad (15)$$

where  $\mathbf{p}_{\text{tot}}$  is the sum of the four momenta  $\mathbf{p}_i$ , and we have suppressed the spin labels on  $U$ . For a generic set of momenta  $\mathbf{p}_i$  the delta function constrains the large components of the momenta and scales as  $\delta^3(\mathbf{p}_{\text{tot}}) \sim s^0$ . In this case the four-fermion interaction scales as  $s^1$  and becomes irrelevant near the Fermi surface. Interactions involving more fermions are even more strongly suppressed.

An exception occurs if the large components of the momenta cancel. This happens for back-to-back momenta,  $\mathbf{k}_1 = -\mathbf{k}_2$ , and for generalized forward scattering,  $\mathbf{k}_1 \cdot \mathbf{k}_2 = \mathbf{k}_3 \cdot \mathbf{k}_4$ . In these cases one component of the delta functions constrains  $\mathbf{l}$ , the scaling of the delta function is changed to  $s^{-1}$ , and the four-fermion interaction is marginal,  $S_{4f} \sim s^0$ . Whether or not the four-fermion interaction qualitatively changes the theory of non-interacting quasi-particles described by Eq. (14) depends on quantum corrections, which can change the scaling from marginal to marginally relevant [ $S_{4f} \sim \log(s)$ ] or irrelevant [ $S_{4f} \sim \log(s)^{-1}$ ].

The one-loop corrections to the four-fermion interaction are given by

$$\delta S_{BCS} \sim \text{diagram 1}, \quad \delta S_{ZS} \sim \text{diagram 2}, \quad \delta S_{ZS'} \sim \text{diagram 3}. \quad (16)$$

There are two possible scenarios. One possibility is that the interaction in the BCS channel ( $\mathbf{k}_1 = -\mathbf{k}_2$ ) is attractive in some partial wave. In this case the first diagram in Eq. (16) leads to a logarithmic growth of the interaction. We can illustrate this effect using the  $s$ -wave four-fermion interaction defined in Eq. (3). For  $\mathbf{p}_1 = -\mathbf{p}_2$  and  $E_1 = E_2 = E$ , the one-loop correction to  $C_0$  is given by

$$-C_0^2 \left( \frac{k_F m}{2\pi^2} \right) \log \left( \frac{E_0}{E} \right), \quad (17)$$

where  $E_0$  is an ultraviolet cutoff. This result can be interpreted as an effective energy-dependent coupling. The coupling constant satisfies the renormalization group equation

$$E \frac{dC_0}{dE} = C_0^2 \left( \frac{k_F m}{2\pi^2} \right) \Rightarrow C_0(E) = \frac{C_0(E_0)}{1 + NC_0(E_0) \log(E_0/E)}, \quad (18)$$

where  $N = k_F m / 2\pi^2$  is the density of states. Equation (18) shows that if the initial coupling is repulsive,  $C_0(E_0) > 0$ , then the renormalization group evolution will drive the effective coupling to zero. If, on the other hand, the initial coupling is attractive,  $C_0(E_0) < 0$ , then the effective coupling grows and reaches a pole (called a “Landau pole”) at  $E_{crit} \sim E_0 \exp(-1/(N|C_0(E_0)|))$ . At the Landau pole the effective theory defined by Eq. (14,15) has to break down. The renormalization group equation does not determine what happens at this point, but it is natural to assume that the strong attractive interaction leads to the formation of a fermion pair condensate in the BCS channel  $\langle \psi(\mathbf{p})\psi(-\mathbf{p}) \rangle$ . The magnitude of the difermion condensate as well as the corresponding gap in the energy spectrum is easiest to compute if the microscopic interaction is weak (if  $k_f R < 1$ ). Employing standard methods we can derive the gap equation

$$1 = \frac{|C_0|}{2} \int \frac{d^3p}{(2\pi)^3} \frac{1}{\sqrt{(E_p - E_F)^2 + \Delta^2}}. \quad (19)$$

The infrared divergence in the BCS channel is regulated by the energy gap  $\Delta$ . The gap equation also has a logarithmic ultraviolet divergence. This divergence can be treated consistently with the relation between  $C_0$  and  $a_0$  derived in Section 2.1 by using dimensional regularization [16,17]. The result is

$$\Delta = \frac{8E_F}{e^2} \exp \left( -\frac{\pi}{2k_F|a_0|} \right). \quad (20)$$

The term in the exponent represents the leading term in an expansion in  $k_F|a_0|$ . This means that in order to determine the pre-exponent in Eq. (20) we have to solve the gap equation at next-to-leading order. This correction corresponds to keeping the ZS (“zero sound”) diagram in Eq. (16). In nuclear physics this term is known as the “induced interaction” [18]. In the case of a zero-range potential the induced interaction was first computed by Gorkov and Melik-Barkhudarov [19]. It leads to a suppression of the  $s$ -wave gap by a factor  $(4e)^{1/3} \simeq 2.2$

For nuclear matter the result given in Eq. (20) is not very useful, both because the scattering length is large, and because effective range corrections are not negligible. We will discuss the pairing



gap in the limit  $a_0 \rightarrow \infty$  in Section 2.3 below. Range corrections in the case of a normal scattering length were studied in [16]. A rough estimate of the gap at moderate densities can be obtained by replacing  $1/(k_F a)$  with  $\cot[\delta_0(k_F)]$ , where  $\delta_0(k)$  is the  $s$ -wave phase shift. This estimate gives neutron gaps on the order of 1 MeV at nuclear matter density.

The second scenario arises if the interaction in the BCS channel is either repulsive or very weak. In this case the forward scattering amplitudes are important. The interaction is

$$U(\hat{p}_4, \hat{p}_3, \hat{p}_2, \hat{p}_1)|_{\hat{p}_1 \cdot \hat{p}_2 = \hat{p}_3 \cdot \hat{p}_4} = F(\hat{p}_1 \cdot \hat{p}_2, \phi_{12,34}) , \quad (21)$$

where  $\phi_{12,34}$  is the angle between the plane spanned by  $\mathbf{p}_{1,2}$  and  $\mathbf{p}_{3,4}$ . The function  $F(x, 0)$  is called the Landau function and its Legendre coefficients are referred to as Landau parameters. If spin-dependence is included there is a second set of Landau parameters commonly denoted  $F'_l$ . The Landau parameters remain marginal at one-loop order.

The effective field theory characterized by  $v_F$  and  $F_l$  is called Landau Fermi liquid theory [11, 12]. The Landau parameters can be related to the compressibility, the velocity of zero and first sound, transport coefficients, etc. The compressibility of nuclear matter, for example, is given by

$$\frac{dP}{d\rho} = \frac{k_F^2}{m^2} \frac{1 + F_0}{3 + F_1} . \quad (22)$$

The coefficients  $F_l$  can be extracted from experiment, but ultimately we would like to find a systematic method for computing the Landau parameters from the underlying nucleon-nucleon interaction. One possibility is to use the renormalization group (RG) to integrate out modes far away from the Fermi surface. A difficulty with this strategy is the problem of finding suitable initial conditions for the RG flow. Brown, Friman, and Schwenk proposed to use a free space RG to generate a universal low momentum effective interaction  $V_{\text{low } k}$  (which we shall discuss in more detail in Section 3.2 below). This interaction, evolved to a scale  $\Lambda \sim 2k_F$ , can be used as a starting point for the determination of the Landau parameters [20].

### 2.3 Unnatural Scattering Length

An important aspect of nuclear physics is the fact that the nucleon scattering lengths are anomalously large. The neutron-proton scattering length in the  $^1S_0$  channel is  $-23.71$  fm, and the binding energy in the  $^3S_1$  (deuteron) channel is 2.2 MeV. This implies that expanding the scattering amplitudes in powers of the momentum [as in Eq. (5)] is not useful, and that powers of  $a_0 k$  have to be kept to all orders. Keeping the first two terms in the effective range expansion, the scattering amplitude can be written as

$$f_0(k) \sim \frac{1}{-1/a_0 + r_0 k^2/2 - ik} = \frac{1}{-1/a_0 - ik} \left\{ 1 + \frac{r_0/2}{-1/a_0 - ik} + \dots \right\} . \quad (23)$$

This expansion can be reproduced by keeping the  $s$ -wave contact interaction proportional to  $C_0$  to all orders, and treating  $C_{2i}$  ( $i > 0$ ) perturbatively as before. This procedure gives the correct result, but in dimensional regularization (with minimal subtraction) or cutoff regularization the power counting of individual diagrams is not manifest. This is easily seen in dimensional regularization where  $C_0 \rightarrow \infty$  as  $a_0 \rightarrow \infty$ . As a consequence, individual diagrams diverge in the limit of a large scattering length even though the sum of all diagrams is finite. Kaplan, Savage, and Wise proposed

a modified version of dimensional regularization (power divergence subtraction, PDS) in which poles in lower dimensions are subtracted, and power counting is manifest [21].

Interest in many-body systems with a large two-particle scattering length arises not only in nuclear physics, but also in atomic physics. It is now possible to create cold atomic gases in which the scattering length  $a_0$  of the atoms can be adjusted experimentally using Feshbach resonances, see [22] for a review. If the density is low the atoms can be described as pointlike nonrelativistic particles that carry a “spin” label which characterizes the hyperfine quantum numbers of the atoms. A Feshbach resonance arises if a molecular bound state in a closed hyperfine channel crosses near the threshold of a lower “open” channel. Because the magnetic moments of the open and closed states are in general different, Feshbach resonances can be tuned using an applied magnetic field. At resonance the two-body scattering length in the open channel diverges, and the cross section  $\sigma$  is limited only by unitarity,  $\sigma(k) = 4\pi/k^2$  for low momenta  $k$ . In the unitarity limit, details about the microscopic interaction are lost, and the system displays universal properties.

A dilute gas of *any* fermions in the unitarity limit is a strongly coupled quantum liquid that exhibits universality. At low density we are interested in the limit  $k_F a_0 \rightarrow \infty$  and  $k_F r_0 \rightarrow 0$ . From dimensional analysis it is clear that the energy per particle at zero temperature has to be proportional to energy per particle of a free Fermi gas at the same density,

$$\frac{E}{A} = \xi \left( \frac{E}{A} \right)_0 = \xi \frac{3}{5} \left( \frac{k_F^2}{2m} \right). \quad (24)$$

The constant  $\xi$  is universal, *i.e.*, independent of the details of the system. Similar universal constants govern the magnitude of the gap in units of the Fermi energy and the equation of state at finite temperature.

Calculating these universal constants is clearly a very challenging task – many-body diagrams containing  $C_0$  have to be summed to all orders. One possibility is to do the calculation numerically, using diffusion or imaginary time path integral Monte Carlo methods as described in Section 3.3. It is also desirable to find systematically improvable analytical approaches. Analytical methods offer the possibility to systematically include higher order terms in the interaction (range corrections, explicit pions, three-body forces, etc.) and to determine real time properties that are hard to access numerically. A number of analytical methods have been considered, such as an expansion in the number of fermion species [23, 24] or the number of spatial dimensions (which is related to the hole-line expansion of Brueckner, Bethe, and Goldstone) [25, 26]. In the following we shall discuss a proposal by Nussinov & Nussinov to perform an expansion around  $d = 4 - \epsilon$  spatial dimensions. Epsilon expansions are well known in the theory of critical phenomena. An interesting aspect of the epsilon expansion in nuclear physics is that both many-body and few-body system can be studied [27].

Nussinov & Nussinov observed that the fermion many-body system in the unitarity limit reduces to a free Fermi gas near  $d = 2$  spatial dimensions, and to a free Bose gas near  $d = 4$  [28]. Their argument was based on the behavior of the two-body wave function as the binding energy goes to zero. For  $d = 2$  it is well known that the limit of zero binding energy corresponds to an arbitrarily weak potential. In  $d = 4$  the two-body wave function at  $a_0 = \infty$  has a  $1/r^2$  behavior and the normalization is concentrated near the origin. This suggests the many-body system is equivalent to a gas of non-interacting bosons. A systematic expansion based on the observation of Nussinov & Nussinov was studied by Nishida and Son [29]. In this section we shall explain their approach.

We begin by restating the argument of Nussinov & Nussinov in the effective field theory language. For simplicity we shall work with dimensional regularization and minimal subtraction. In this case  $a_0 \rightarrow \infty$  corresponds to  $C_0 \rightarrow \infty$ . The fermion-fermion scattering amplitude is given by

$$f(p_0, \mathbf{p}) = \left(\frac{4\pi}{m}\right)^{d/2} \left[\Gamma\left(1 - \frac{d}{2}\right)\right]^{-1} \frac{i}{(-p_0 + E_p/2 - i\delta)^{\frac{d}{2}-1}}, \quad (25)$$

where  $\delta \rightarrow 0+$ . As a function of  $d$  the Gamma function has poles at  $d = 2, 4, \dots$  and the scattering amplitude vanishes at these points. Near  $d = 2$  the scattering amplitude is energy and momentum independent. For  $d = 4 - \epsilon$  we find

$$f(p_0, \mathbf{p}) = \frac{8\pi^2\epsilon}{m^2} \frac{i}{p_0 - E_p/2 + i\delta} + \mathcal{O}(\epsilon^2). \quad (26)$$

We observe that at leading order in  $\epsilon$  the scattering amplitude looks like the propagator of a boson with mass  $2m$ . The boson-fermion coupling is  $g^2 = (8\pi^2\epsilon)/m^2$  and vanishes as  $\epsilon \rightarrow 0$ . This suggests that we can set up a perturbative expansion involving fermions of mass  $m$  weakly coupled to bosons of mass  $2m$ . A difermion field can be introduced using the Hubbard-Stratonovich trick. The difermion self-coupling is proportional to  $1/C_0$  and vanishes in the unitarity limit. The Lagrangian is

$$\mathcal{L} = \Psi^\dagger \left[ i\partial_0 + \sigma_3 \frac{\nabla^2}{2m} \right] \Psi + \mu \Psi^\dagger \sigma_3 \Psi + \left( \Psi^\dagger \sigma_+ \Psi \phi + \text{h.c.} \right), \quad (27)$$

where  $\Psi = (\psi_\uparrow, \psi_\downarrow)^T$  is a two-component Nambu-Gorkov field,  $\sigma_i$  are Pauli matrices acting in the Nambu-Gorkov space and  $\sigma_\pm = (\sigma_1 \pm i\sigma_2)/2$ .

In the superfluid phase  $\phi$  acquires an expectation value. We write

$$\phi = \phi_0 + g\varphi, \quad g = \frac{\sqrt{8\pi^2\epsilon}}{m} \left( \frac{m\phi_0}{2\pi} \right)^{\epsilon/4}, \quad (28)$$

where  $\phi_0 = \langle \phi \rangle$ . The scale  $M^2 = m\phi_0/(2\pi)$  was introduced in order to have a correctly normalized boson field. The scale parameter is arbitrary, but this particular choice simplifies some of the algebra. In order to get a well-defined perturbative expansion we add and subtract a kinetic term for the boson field to the Lagrangian. We include the kinetic term in the free part of the Lagrangian

$$\mathcal{L}_0 = \Psi^\dagger \left[ i\partial_0 + \sigma_3 \frac{\nabla^2}{2m} + \phi_0(\sigma_+ + \sigma_-) \right] \Psi + \varphi^\dagger \left( i\partial_0 + \frac{\nabla^2}{4m} \right) \varphi, \quad (29)$$

and the interacting part is

$$\mathcal{L}_I = g \left( \Psi^\dagger \sigma_+ \Psi \varphi + \text{h.c.} \right) + \mu \Psi^\dagger \sigma_3 \Psi - \varphi^\dagger \left( i\partial_0 + \frac{\nabla^2}{4m} \right) \varphi. \quad (30)$$

Note that the interacting part generates self-energy corrections to the boson propagator which, by virtue of Eq. (26), cancel against the kinetic term of boson field. We have also included the chemical potential term in  $\mathcal{L}_I$ . This is motivated by the fact that near  $d = 4$  the system reduces to a non-interacting Bose gas and  $\mu \rightarrow 0$ . We will count  $\mu$  as a quantity of  $\mathcal{O}(\epsilon)$ .

The Feynman rules are quite simple. The fermion and boson propagators are

$$G(p_0, \mathbf{p}) = \frac{i}{p_0^2 - E_p^2 - \phi_0^2} \begin{bmatrix} p_0 + E_p & -\phi_0 \\ -\phi_0 & p_0 - E_p \end{bmatrix}, \quad D(p_0, \mathbf{p}) = \frac{i}{p_0 - E_p/2}, \quad (31)$$

and the fermion-boson vertices are  $ig\sigma_{\pm}$ . Insertions of the chemical potential are  $i\mu\sigma_3$ . Both  $g^2$  and  $\mu$  are corrections of order  $\epsilon$ . There are a finite number of one-loop diagrams that generate  $1/\epsilon$  terms. All other diagrams are finite, and the  $\epsilon$  expansion is well defined.

The ground-state energy is determined by diagrams with no external legs. The first diagram is the free fermion loop which is  $\mathcal{O}(1)$  in the epsilon expansion. We get

$$\text{Feynman diagram: circle with arrows} = - \int \frac{d^d p}{(2\pi)^d} \sqrt{E_p^2 + \phi_0^2} = \frac{\phi_0}{3} \left[ 1 + \frac{7 - 3(\gamma + \log(2))}{6} \epsilon \right] \left( \frac{m\phi_0}{2\pi} \right)^{d/2}. \quad (32)$$

An insertion of  $\mu$  is also  $\mathcal{O}(1)$  because the loop diagram is divergent in  $d = 4$ . We find

$$\text{Feynman diagram: circle with arrows and a cross} = \mu \int \frac{d^d p}{(2\pi)^d} \frac{E_p}{\sqrt{E_p^2 + \phi_0^2}} = -\frac{\mu}{\epsilon} \left[ 1 + \frac{1 - 2(\gamma - \log(2))}{4} \epsilon \right] \left( \frac{m\phi_0}{2\pi} \right)^{d/2}. \quad (33)$$

Graphs with extra insertions of  $\mu$  follow the naive epsilon counting and are at least  $\mathcal{O}(\epsilon^2)$ . Nishida and Son also computed the leading two-loop contribution which is  $\mathcal{O}(\epsilon)$  because of the factor of  $g^2$  from the vertices. The result is

$$\text{Feynman diagram: circle with arrows and a dashed line} = -C\epsilon \left( \frac{m\phi_0}{2\pi} \right)^{d/2}, \quad (34)$$

where the dashed line denotes the difermion propagator, and  $C \simeq 0.14424$ .

We can now determine the minimum of the effective potential. We find  $\phi_0 = (2\mu)/\epsilon(1 + C'\epsilon + \mathcal{O}(\epsilon^2))$  with  $C' = 3C - 1 + \log(2)$ . The value of the effective potential at  $\phi_0$  determines the pressure and  $n = \partial P/\partial\mu$  gives the density. From the density we can compute the Fermi momentum ( $n \sim k_F^d$  in  $d$  dimensions), and the relationship between the Fermi energy  $\varepsilon_F = k_F^2/2m$  and  $\mu$  determines the universal parameter  $\xi = \mu/\varepsilon_F$ . We find

$$\xi = \frac{1}{2}\epsilon^{3/2} + \frac{1}{16}\epsilon^{5/2}\log(\epsilon) - 0.025\epsilon^{5/2} + \dots = 0.475 \quad (\epsilon = 1), \quad (35)$$

which agrees quite well with the result of fixed-node quantum Monte Carlo calculations. The calculation was extended to  $\mathcal{O}(\epsilon^{7/2})$  by Arnold et al. [30]. Unfortunately, the next term is very large and it appears necessary to combine the expansion in  $4 - \epsilon$  dimensions with a  $2 + \epsilon$  expansion in order to extract useful results. The  $\epsilon$  expansion has also been applied to the calculation of the gap [29]. At next-to-leading order the result is  $\Delta = 0.62\varepsilon_F$ . Somewhat surprisingly, this result is quite close to the naive  $a_0 \rightarrow \infty$  limit of the BCS result Eq. (20), provided the induced interaction term is taken into account.

### 3 EFT FOR FINITE NUCLEI AND NUCLEAR MATTER

In this section, we survey the wide range of pioneering applications of EFT to nonrelativistic finite density nuclear systems. These frontiers are rapidly evolving and most results are immature, so we focus on general illustrative aspects.

#### 3.1 Pion Physics From Chiral EFT

To apply EFT to finite nuclei and nuclear matter, we must first consider the appropriate degrees of freedom. Applications to sufficiently low-density systems such as dilute neutron matter are possible

with nucleons only. These are called “pionless” effective field theories. In such an EFT, the pion is a heavy degree of freedom whose effects are mimicked by contact terms. This EFT breaks down when external momenta are comparable to the pion mass, so that pion exchange is resolved. This does not automatically translate into a clear limit on its applicability to finite nuclei; pionless EFT is successful for at least the ground states of the deuteron and triton and its limits for heavier nuclei are not yet known [4].

However, given that the Fermi momentum  $k_F$  for the interior of heavy nuclei is about twice the pion mass, one expects the pion must be treated as a long-range degree-of-freedom in a free-space EFT applicable to most nuclei. Chiral effective field theories for nucleons incorporate the pion systematically as the (near) Goldstone boson of approximate and spontaneously broken chiral symmetry, expanding about the massless pion limit. The functional dependence on the QCD quark masses is captured in perturbation theory and the dependence on the strong coupling is contained in universal parameters to be determined from data or direct numerical calculations of QCD. Chiral EFT in nuclear physics originated with the seminal work of Weinberg and van Kolck and collaborators in the early 1990’s [31,32,33,34,35,36,37], and there has been active development ever since [5,4,6].

The most commonly applied chiral EFT Lagrangians at present have nonrelativistic nucleons and pions as degrees of freedom based on the “heavy-baryon” formalism, which eliminates anti-nucleons and organizes relativistic corrections [4]. As usual, renormalization can be carried out because all interactions consistent with QCD symmetries are included, which allows regulator dependence to be absorbed. To organize the EFT in a systematic hierarchy we need a power counting but the optimal scheme is not yet settled. Both practical and formal questions are being argued and different schemes are under investigation [38,39,40,41]. In all cases, chiral symmetry dictates that pion interactions are accompanied by derivatives (because they are Goldstone bosons) or powers of the pion mass (Ward identity constraints from QCD), which then yields ratios of characteristic momenta and  $m_\pi$  to the scale of excluded physics, such as heavier meson exchange, as expansion parameters. Relativistic corrections are organized in powers momenta over the nucleon mass.

For applications to nuclear structure, an energy-independent nucleons-only potential is desirable (and required for many of the methods discussed below); it can be derived from the chiral Lagrangian by a unitary transformation method that decouples the nucleons from *explicit* pion fields, leaving static pion-exchange interactions and regulated contact terms [6]. At present these potentials are organized by a power counting proposed by Weinberg and then iterated with a Lippmann-Schwinger equation for two-body scattering or other nonperturbative methods for bound-state properties with more nucleons. A momentum-space cutoff is used for technical reasons, which means the advantages of dimensional regularization we saw for short-range interactions at finite density are not available.

For Weinberg power counting there is a formula analogous to Eq. (11) that identifies the order in the EFT expansion at which a given term in the potential contributes. This yields a hierarchy of terms with increasing derivatives and pion exchanges and, perhaps most important for finite density applications to be tractable, a hierarchy of many-body forces. At leading order (LO), there is one-pion exchange and two no-derivative contact terms. The next-to-leading-order (NLO) adds the first two-pion exchange contributions, which are important for the mid-range nuclear attraction. At present, NN interactions go to up to  $N^3\text{LO}$ , which includes 24 constants for the contact terms

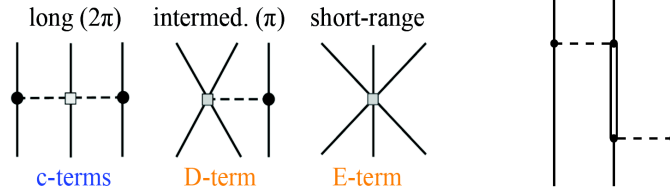


Figure 1: Leading three-body contributions in chiral EFT. Left:  $N^2$ LO terms in a EFT without  $\Delta$ 's (dashed line is the pion). Right: NLO contribution with explicit  $\Delta$ 's (double line).

(not including isospin violation) that are determined by fits to NN scattering. The best fits have a  $\chi^2/\text{dof}$  comparable to the best phenomenological potentials [42, 43].

Three-nucleon forces (3NF) appear first at  $N^2$ LO and are shown on the left in Fig. 1. There are parameters associated with long-range two-pion exchange (four constants fit to  $\pi N$  or  $NN$  scattering), mid-range one-pion exchange (one constant), and purely short-range (one constant) parts. The extension to  $N^3$ LO is in progress and involves many additional diagrams but no additional parameters. However, there are sizable uncertainties at present in determining the long-range 3NF parameters from  $\pi N$  or  $NN$  scattering, which translates into significant uncertainties at finite density. The 4N interaction appears first at  $N^3$ LO in the form of long-range pion exchange and is parameter free [44]. The quantitative suppression of many-nucleon forces predicted by chiral power counting is consistent with binding-energy calculations in light nuclei [6, 45], but much remains to be tested in larger systems.

Even after we have specified a power counting and the order in the expansion, there is not a unique EFT potential because one can choose different cutoffs. Calculations of observables should be independent of the cutoff at the level of the truncation error determined by the missing orders. By comparing calculations with varied cutoffs one can test whether the EFT is working and put a bound on the theoretical error. The precision EFT potentials currently available for nuclear structure have cutoffs in a rather narrow range close to the expected breakdown scale of the EFT, about 450–600 MeV (*cf.* the  $\rho$  or  $\omega$  meson mass), which is consistent with the prescription of Lepage [46, 47]. In practice, lower cutoffs would mean large truncation errors (*i.e.*, the expansion parameter  $q/\Lambda_c$  gets too small) while larger cutoffs create implementation problems with increasingly singular (at short distances) potentials from multiple pion exchange. Within this cutoff range there is no penalty for iterating sub-leading potential terms, which violates some power countings, because the truncation and iteration errors are the same size [4].

Recent surveys of on-going applications of chiral potentials to scattering and to properties of few-body nuclei can be found in Refs. [4, 6]. Among the developments most relevant to finite density is work to add the  $\Delta(1232)$ -isobar resonance explicitly to the chiral EFT Lagrangian; this was part of the original explorations by van Kolck *et al.*, but has only recently been reconsidered for energy-independent potentials [48, 49]. The  $\Delta$  is considered important because of its low-excitation energy (the mass difference to the nucleon is about 300 MeV) and its strong coupling to the  $\pi N$  system. Including it would resum important contributions and improve the pattern of convergence. In this scheme, the leading 3NF term comes from pion exchange with an intermediate  $\Delta$  (right diagram in Fig. 1) and appears at NLO. As this and other developments mature, in parallel there will be

applications to finite nuclei. Indeed, since the energy-independent potentials take the same form as phenomenological non-local potentials, almost all conventional few- and many-body methods are immediately available.

### 3.2 Wave Function Methods

There are a wide variety of methods available to determine properties of few-body systems given an internucleon potential. These all in some way involve solving for the approximate wave function of the system. If we arbitrarily set the cross-over from few-body to many-body nuclei at  $A = 8$ , the choice of methods dwindles to a few: Green’s function Monte Carlo (GFMC), no-core shell model (NCSM), and coupled cluster (CC). The GFMC approach [50, 51] has had great success up to  $A = 12$  (and extensions using auxiliary field methods promise to go much further), but is limited at present to local potentials, *i.e.*, diagonal in coordinate representation, which excludes current chiral EFT interactions. However, both NCSM and CC methods are compatible with energy-independent chiral potentials including many-body forces [52, 53].

The NCSM diagonalizes the Hamiltonian in a harmonic oscillator basis with all nucleons active (hence “no core”). Lanczos methods allow the extraction of the lowest eigenvalues and eigenvectors from spaces up to dimension  $10^9$  (and growing with computer hardware and software advances), but the matrix size grows rapidly with  $A$  and the maximum oscillator excitation energy  $N_{\max} \hbar \Omega$ . For a given  $A$ , the convergence of observables with  $N_{\max}$  depends strongly on the nature of the potential. Chiral EFT Hamiltonians are softer than conventional nuclear potentials (*i.e.*, smaller high-momentum contributions, which means less coupling to high oscillator states), but adequate convergence with 3NF still requires too large a basis beyond the lightest nuclei. Therefore Lee-Suzuki transformations of the potential, which are unitary order-by-order in a cluster expansion, are applied to decouple included and excluded oscillator states, greatly reducing the size of the model space needed. This procedure has many demonstrated successes [52, 54] although there are drawbacks, such as distortions of long-range physics, problems with extrapolations of energies, and the loss of the variational principle [55].

Recent state-of-the-art NCSM calculations of excitation energies for four  $p$ -shell nuclei are shown in Fig. 2 for a single  $N^3\text{LO}$  potential with and without the  $N^2\text{LO}$  3NF [54]. (The mismatch in orders means that this calculation is not yet completely consistent from the EFT perspective.) It is evident that the fine structure of the nuclear spectra is uniformly improved with the three-body contribution. Of particular note is the ground state of  $^{10}\text{B}$  and the splittings of spin-orbit partners throughout. The sensitivity of three-body parameters to particular observables (*e.g.*,  $^6\text{Li}$  quadrupole moment, the lowest  $1^+$  states in  $^{10}\text{B}$ ) suggests that fits of 3NF parameters will improve with input from more than  $A = 3, 4$  systems [54].

How do we tell if an EFT-based interaction used by a wave function method is working as advertised? One way is to do comparative calculations at different orders in the EFT with a range of cutoffs. Since cutoff variation is absorbed by the contact interactions, which scale as powers of the inverse cutoff, the relative variation of the potential energies over this range should decrease systematically according to the power of omitted contact interactions (and assuming a typical momentum scale  $\approx 130\text{ MeV}$ ). Binding energy variations will be larger because of cancellations in nuclear systems, which amplify the role of higher orders (including many-body forces). Nogga has

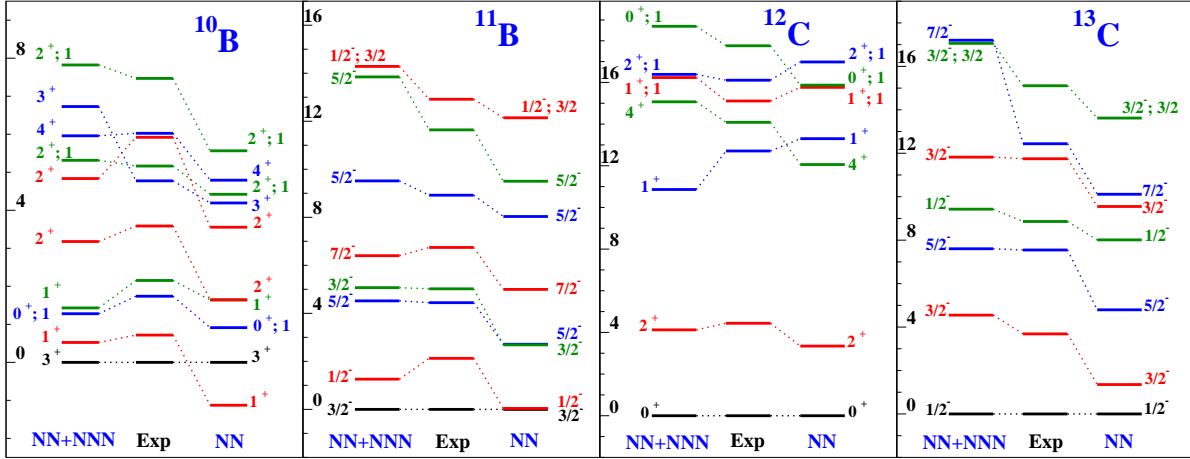


Figure 2: Excitation energies (in MeV) of selected levels in four  $p$ -shell nuclei [54] calculated using the  $N^3\text{LO}$  potential of Ref. [42]. Calculations with NN-only and with  $N^3\text{LO}$  NN plus  $N^2\text{LO}$  3NF are compared to experiment.

shown that such estimates are consistent with calculations in  $^3\text{H}$  [56]. For  $^4\text{He}$ , he concludes that the EFT estimate of 2% for the ratio of 3NF to NN potential energies is consistent with observed ratios of roughly 5% [56] and preliminary calculations of the 4NF contribution were found to be as small as expected [45]. All of these tests will need to be repeated for larger nuclei as reliable calculations become possible.

Renormalization group (RG) methods applied in free space to chiral EFT interactions are a promising avenue to calculating larger nuclei. These methods prescribe how each matrix element of the potential (and other operators) in a discretized momentum basis must evolve under changes in the “resolution scale” so that observables are unchanged. (Since the potential is not an observable, we are always free to make unitary transformations.) The resolution scale is changed by lowering a cutoff in relative momentum (“ $V_{\text{low } k}$ ” [57]) or using a flow equation for the Hamiltonian (“similarity RG” [58]) or by tailored unitary transformations (“UCOM” [59]). The result is a decoupling of high- and low-momentum dependence without modifying long-distance interactions, leading to low-momentum potentials that are more perturbative, such that convergence in harmonic oscillator bases is dramatically accelerated [60]. Such potentials can be applied without Lee-Suzuki transformations in the NCSM and maintain the variational principle. Since the transformations are unitary, the EFT truncation error is unchanged, in contrast to the RG evolution of a chiral EFT at fixed order to low cutoff. However, the evolution of the NN potential is inevitably accompanied by the evolution of the three- and higher-body potentials. The latter is not yet implemented but is instead approximated by fitting the  $N^2\text{LO}$  chiral interaction at each cutoff [61], which introduces a theoretical error.

These low-momentum potentials show great promise for the CC method, which has been highly developed in *ab initio* quantum chemistry but only recently revived for nuclear applications, including the development of CC theory for three-body Hamiltonians [62,53]. Coupled cluster calculations are based on a potent exponential ansatz for the ground-state wave function,  $|\psi\rangle = e^{\hat{T}}|\phi\rangle$ , where  $|\phi\rangle$  is a simple reference state, typically a harmonic oscillator Slater determinant. The operator



$\hat{T}$  is specified by amplitudes for a truncated sum of operators creating one-particle–one-hole, two-particle–two-hole, *etc.* excitations. The amplitudes are found from nonlinear equations whose solution scales very gently with the size of the nucleus and model space.

As with the NCSM, convergence is accelerated with low-momentum potentials and particularly promising is the calculation of 3NF contributions, which are the most expensive component. The 3NF potential is rewritten in terms of normal-ordered creation and destruction operators with respect to  $|\phi\rangle$  (instead of the vacuum), which recasts the 3NF into an expectation value in  $|\phi\rangle$ , one- and two-body pieces, and the remaining 3NF part. In the hierarchy of contributions to a CC calculation, only the last piece is expensive to calculate, but recent CC calculations of  ${}^4\text{He}$  found it to be negligible [53]. If this results persists for larger nuclei, calculations of  $A = 100$  or beyond will be feasible in the near future! The present limit for NCSM is much lower, around  $A = 16$  but could be extended using importance sampling methods that pick out the most important basis states [63], if they can be implemented in a size-extensive way.

The NCSM and CC wave function methods apply EFT (and RG) only to create the input potential and not in solving the many-body problem. There is also the possibility of a more EFT-like treatment, such as the pioneering work to apply EFT to the shell model by Stetcu, Barrett and van Kolck [64]. (See Ref. [65] for a completely different application of EFT methods to the shell model.) These authors formulate an EFT in the harmonic oscillator basis, where the restricted model space generates all interactions consistent with the underlying symmetries. The parameters are directly determined in the model space rather than fitting in free space and transforming the interaction. The oscillator frequency sets an infrared cutoff  $\lambda \sim \sqrt{M_N \hbar \Omega}$  while the ultraviolet cutoff is  $\Lambda \sim \sqrt{M_N(N_{\text{max}} + 3/2)\hbar\Omega}$ . Within each model space, a set of observables is used to fix the EFT parameters and then other observables are calculated. The EFT works if cutoff dependence decreases with decreasing  $\lambda$  and increasing  $\Lambda$ ; in that case an extrapolation to the continuum limit  $\hbar\Omega \rightarrow 0$  with  $N_{\text{max}} \rightarrow 0$  with  $\Lambda$  fixed is made. At the end, one takes  $\Lambda \rightarrow \infty$ . The first application with a pionless theory up to  $A = 6$  is encouraging and motivates generalizations to the pionful theory and to other many-body methods [64].

### 3.3 EFT on the Lattice

We have seen that chiral effective field theory potentials have been used successfully in connection with standard numerical many-body approaches such as coupled cluster or the no-core shell model. A disadvantage of these methods is that they rely on the existence of a potential, which is not an observable, and as a consequence scheme and renormalization scale invariance are not manifest. A numerical few and many-body method that is based directly on the effective Lagrangian is the euclidean lattice path integral Monte Carlo method. Euclidean lattice calculations are standard in the context of QCD but, except for some isolated attempts [66,67], have been introduced in nuclear physics only recently [68,69,70].

In the following we shall introduce the method in the case of a simple  $s$ -wave contact interaction  $\mathcal{L} = -C_0(\psi^\dagger\psi)^2/2$ . More sophisticated interactions involving higher partial wave terms and explicit pions are discussed in [71]. The usual strategy for dealing with the four-fermion interaction is to

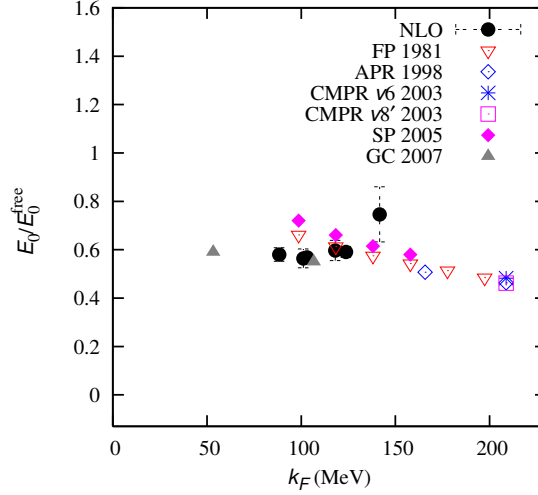


Figure 3: Lattice results for the energy per particle of a dilute Fermi gas from Borasoy *et al.* [71]. We show the energy per particle in units of the energy per particle of the free system as a function of the Fermi momentum. The solid dots are the lattice results. For comparison, we also show results from wave-function-based many-body calculations (see [71]).

use a Hubbard-Stratonovich transformation. The partition function can be written as [68]

$$Z = \int Ds Dc Dc^* \exp[-S] , \quad (36)$$

where  $s$  is the Hubbard-Stratonovich field and  $c$  is a Grassmann field.  $S$  is a discretized euclidean action

$$S = \sum_{\mathbf{n}, i} \left[ e^{-\hat{\mu}\alpha_t} c_i^*(\mathbf{n}) c_i(\mathbf{n} + \hat{\mathbf{0}}) - e^{\sqrt{-C_0\alpha_t}s(\mathbf{n}) + \frac{C_0\alpha_t}{2}} (1 - 6h) c_i^*(\mathbf{n}) c_i(\mathbf{n}) \right] - h \sum_{\mathbf{n}, \mathbf{l}_s, i} \left[ c_i^*(\mathbf{n}) c_i(\mathbf{n} + \hat{\mathbf{l}}_s) + c_i^*(\mathbf{n}) c_i(\mathbf{n} - \hat{\mathbf{l}}_s) \right] + \frac{1}{2} \sum_{\mathbf{n}} s^2(\mathbf{n}). \quad (37)$$

Here  $i$  labels spin and  $\mathbf{n}$  labels lattice sites. Spatial and temporal unit vectors are denoted by  $\hat{\mathbf{l}}_s$  and  $\hat{\mathbf{0}}$ , respectively. The temporal and spatial lattice spacings are  $b_\tau$  and  $b$ , and the dimensionless chemical potential is given by  $\hat{\mu} = \mu b_\tau$ . We define  $\alpha_t$  as the ratio of the temporal and spatial lattice spacings and  $h = \alpha_t/(2\hat{m})$ . The action (37) is quadratic in the fermion fields, and can be simulated using a variety of methods such as determinant or hybrid Monte Carlo. Note that for  $C_0 < 0$  the action is real and importance sampling is possible.

The four-fermion coupling is fixed by computing the sum of all particle-particle bubbles as in Section 2.3 but with the elementary loop function regularized on the lattice. Schematically,

$$\frac{m}{4\pi a_0} = \frac{1}{C_0} + \frac{1}{2} \sum_{\mathbf{p}} \frac{1}{E_{\mathbf{p}}}, \quad (38)$$

where the sum runs over discrete momenta on the lattice and  $E_{\mathbf{p}}$  is the lattice dispersion relation. A detailed discussion of the lattice regularized scattering amplitude can be found in [72, 73, 68].

For a given scattering length  $a_0$  the four-fermion coupling is a function of the lattice spacing. The continuum limit correspond to taking the temporal and spatial lattice spacings  $b_\tau, b$  to zero

$$b_\tau \mu \rightarrow 0, \quad b n^{1/3} \rightarrow 0, \quad (39)$$

keeping  $a_0 n^{1/3}$  fixed. Here,  $\mu$  is the chemical potential and  $n$  is the density. Numerical results for the energy per particle of dilute neutron matter are shown in Fig. 3. We observe that the results agree quite well with traditional many-body calculations. We also note that even with higher-order corrections taken into account, the equation of state exhibits approximate universal behavior, with an effective  $\xi \simeq (0.5\text{--}0.6)$ . For applications of the lattice method to finite nuclei, see [74].

### 3.4 Perturbative EFT for Nuclear Matter

The nuclear calculations discussed so far have all been nonperturbative. However, renormalization group (RG) methods have been used to show that the perturbativeness of internucleon interactions depends strongly on the momentum cutoff and the density [57, 75]. Lowering the resolution via an RG evolution leaves observables and EFT truncation errors unchanged by construction (up to approximation errors and omitted many-body contributions) but shifts contributions between the potential and the sums over intermediate states in loop integrals. These shifts can weaken or even eliminate sources of non-perturbative behavior such as strong short-range repulsion (*e.g.*, from singular chiral two-pion exchange) or the tensor force. At sufficient density, effective range corrections and beyond suppress the effects of large  $s$ -wave scattering lengths [76].

As a consequence, while nuclear matter is generally considered to be nonperturbative, this is also resolution dependent. Figure 4 shows the energy per particle in nuclear matter for several values of the RG cutoff  $\Lambda$  calculated in leading order (Hartree-Fock) and second-order many-body perturbation theory [76]. (Note: The initial potential used in these figures is not a chiral EFT

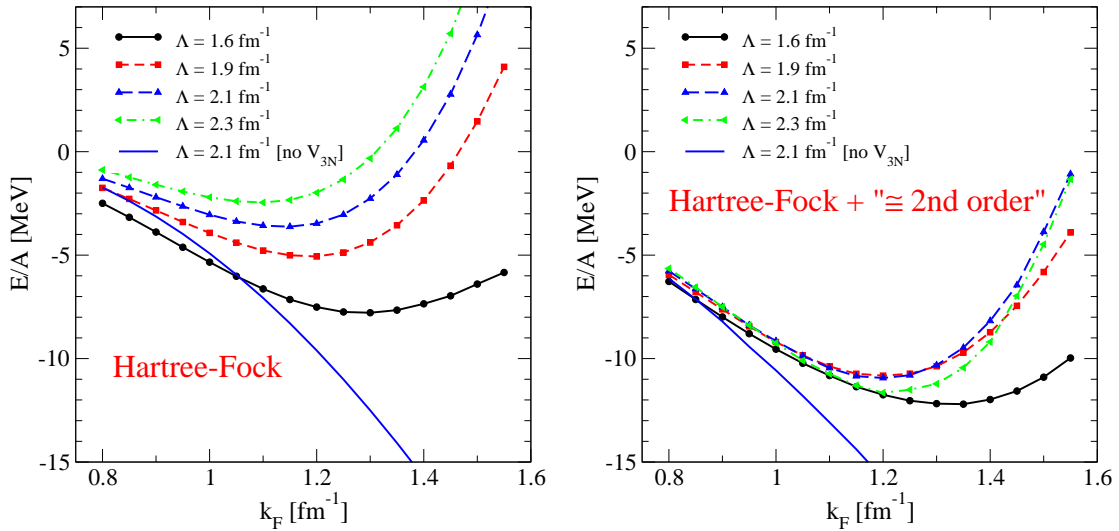


Figure 4: Nuclear matter energy per particle using renormalization-group evolved low-momentum potentials with a range of cutoffs with 3NF fit to few-body binding energies [76]. Left: Hartree-Fock. Right: Hartree-Fock plus second order in the potential.

NN potential. However, all NN potentials fit to scattering phase shifts flow to very similar low-momentum potentials by this range of cutoffs so similar results are expected.) The three-body potential is of the  $N^2\text{LO}$  form, fit at each cutoff to the binding energies of the triton and  $^4\text{He}$ . Since the RG only changes short-distance physics, this is argued to be a good approximation to the consistently evolved 3NF [61].

There are several encouraging features. First, Hartree-Fock is a reasonable starting point for the description of nuclear matter; this is patently false for conventional phenomenological potentials, which do not even bind. Second, the dependence on the cutoff is greatly reduced going to second order. Further calculations show that the third-order ladder diagrams make a very small contribution [76]. Third, with a fit to few-body properties, the minimum is reasonably close to the empirical saturation point of (roughly)  $-16\text{ MeV}$  per particle with  $k_F \approx 1.35\text{ fm}^{-1}$  (indeed, the discrepancy is the order of uncertainties in the three-body force). These results motivate a program to study nuclear matter with chiral EFT internucleon forces evolved to lower resolution (which should also include studying unevolved chiral EFT potentials fit with a lower cutoff).

The increased perturbativeness in nuclear matter with increased density and lower cutoff can be understood physically from reduced phase space due to Pauli blocking and the cutoff, combined with the favorable momentum dependence of the low-momentum interaction [75,76]. Pauli blocking means that particles with momenta below  $k_F$  must forward scatter (Hartree-Fock) or be excited out of the Fermi sea. The latter amplitude is limited by the weakened coupling of occupied and unoccupied states that limits the volume of available momentum states (this is the phase space restriction). A consequence is that the saturation mechanism is now dominated by the three-body force contribution (*cf.* the NN-only curves in the figure), rather than from the density dependence of two-body tensor contributions. For cutoffs in the range shown, the three-body contribution still remains natural-sized according to chiral EFT power counting [76], but is clearly quantitatively important. The implication is that the 4NF contribution will also be important at the level of about an MeV per particle at saturation, but this has yet to be tested.

These results suggest that an alternative EFT power counting may be appropriate at nuclear matter densities. Kaiser and collaborators have proposed a perturbative chiral EFT approach to nuclear matter and then to finite nuclei through an energy functional [77,78,79] (see also [80]). They consider Lagrangians both for nucleons and pions and for nucleons, pions, and  $\Delta$ 's, and fit parameters to nuclear saturation properties. They construct a loop expansion for the nuclear matter energy per particle, which leads to an energy expansion of the form

$$E(k_F) = \sum_{n=2}^{\infty} k_F^n f_n(k_F/m_\pi, \Delta/m_\pi), \quad [\Delta = M_\Delta - M_N \approx 300\text{ MeV}] \quad (40)$$

where each  $f_n$  is determined from a finite number of in-medium Feynman diagrams. All powers of  $k_F/m_\pi$  and  $\Delta/m_\pi$  are kept in the  $f_n$ 's because these ratios are not small quantities [81]. A semi-quantitative description of nuclear matter is found even with just the lowest two terms without  $\Delta$ 's and adding  $\Delta$ 's brings uniform improvement (e.g., in the neutron matter equation of state). There are open questions about power counting and convergence, but many promising avenues to pursue.

### 3.5 Density Functional Theory as an EFT

Density functional theory (DFT) [82,83,84] is widely used in condensed matter and quantum chemistry to treat large many-body systems. It is based on the response of the ground-state energy to external perturbations of the density, with fermion densities as the fundamental variables. This means that the computational cost for DFT is far less than for wave function methods and the calculations can be applied to heavy nuclei. DFT is naturally formulated in an effective action framework [85] and carried out using an inversion method implemented with EFT power counting [86,87,88].

The simple prototype EFT from Section 2 for a dilute system can be revisited in DFT by putting the fermions in a trap potential  $v_{\text{ext}}(\mathbf{x})$  (*e.g.*, a harmonic oscillator) and adding sources coupled to external densities [89]. Consider a single external source  $J(\mathbf{x})$  coupled to the density operator  $\hat{\rho}(x) \equiv \psi^\dagger(x)\psi(x)$  in the partition function (neglecting normalization and factors of the temperature and volume and suppressing  $v_{\text{ext}}$ ),

$$\mathcal{Z}[J] = e^{-W[J]} \sim \text{Tr} e^{-\beta(\hat{H}+J\hat{\rho})} \sim \int \mathcal{D}[\psi^\dagger] \mathcal{D}[\psi] e^{-\int [\mathcal{L}+J\psi^\dagger\psi]} , \quad (41)$$

with the Lagrangian from Section 2.1. The static density  $\rho(\mathbf{x})$  in the presence of  $J(\mathbf{x})$  is

$$\rho(\mathbf{x}) \equiv \langle \hat{\rho}(\mathbf{x}) \rangle_J = \frac{\delta W[J]}{\delta J(\mathbf{x})} , \quad (42)$$

which we invert to find  $J[\rho]$  and then Legendre transform from  $J$  to  $\rho$ :

$$\Gamma[\rho] = -W[J] + \int d^3x J(\mathbf{x})\rho(\mathbf{x}) \quad \text{with} \quad J(\mathbf{x}) = \frac{\delta \Gamma[\rho]}{\delta \rho(\mathbf{x})} \longrightarrow \left. \frac{\delta \Gamma[\rho]}{\delta \rho(\mathbf{x})} \right|_{\rho_{\text{gs}}(\mathbf{x})} = 0 . \quad (43)$$

For static  $\rho(\mathbf{x})$ ,  $\Gamma[\rho]$  is proportional to the Hohenberg-Kohn energy functional, which by Eq. (43) is extremized at the ground state density  $\rho_{\text{gs}}(\mathbf{x})$ .

With  $W[J]$  constructed as a diagrammatic expansion, EFT power counting gives us a means to invert from  $W[J]$  to  $\Gamma[\rho]$  [86,87]. It proceeds by substituting the decomposition  $J(\mathbf{x}) = J_0(\mathbf{x}) + J_1(\mathbf{x}) + J_2(\mathbf{x}) + \dots$  (where “1” means LO, “2” means NLO, and so on) and corresponding expansions for  $W$  and  $\Gamma$  into Eq. (43) and matching order-by-order with  $\rho$  treated as order unity. Here  $J_0$  is chosen so that there are no corrections to the zeroth order density at each order in the expansion; the interpretation is that  $J_0$  is the external potential that yields for a noninteracting system the exact density. Zeroth order is the noninteracting system with potential  $J_0(\mathbf{x})$ ,

$$\Gamma_0[\rho] = -W_0[J_0] + \int d^3x J_0(\mathbf{x})\rho(\mathbf{x}) \implies \rho(\mathbf{x}) = \frac{\delta W_0[J_0]}{\delta J_0(\mathbf{x})} , \quad (44)$$

which is the so-called Kohn-Sham system with the exact density! To evaluate  $W_0[J_0]$ , we introduce orbitals  $\{\psi_\alpha\}$  satisfying (with  $v_{\text{ext}}$  made explicit)

$$\left[ -\frac{\nabla^2}{2M} + v_{\text{ext}}(\mathbf{x}) - J_0(\mathbf{x}) \right] \psi_\alpha(\mathbf{x}) = \varepsilon_\alpha \psi_\alpha(\mathbf{x}) , \quad (45)$$

which diagonalize  $W_0$ , so that it yields a sum of  $\varepsilon_\alpha$ ’s for the occupied states. We calculate the  $W_i$ ’s and  $\Gamma_i$ ’s up to a given order as functionals of  $J_0$  and then determine  $J_0$  for the ground state via a self-consistency loop:

$$J_0 \rightarrow W_1 \rightarrow \Gamma_1 \rightarrow J_1 \rightarrow W_2 \rightarrow \Gamma_2 \rightarrow \dots \implies J_0(\mathbf{x})|_{\rho=\rho_{\text{gs}}} = \left. \frac{\delta \Gamma_{\text{interacting}}[\rho]}{\delta \rho(\mathbf{x})} \right|_{\rho=\rho_{\text{gs}}} . \quad (46)$$

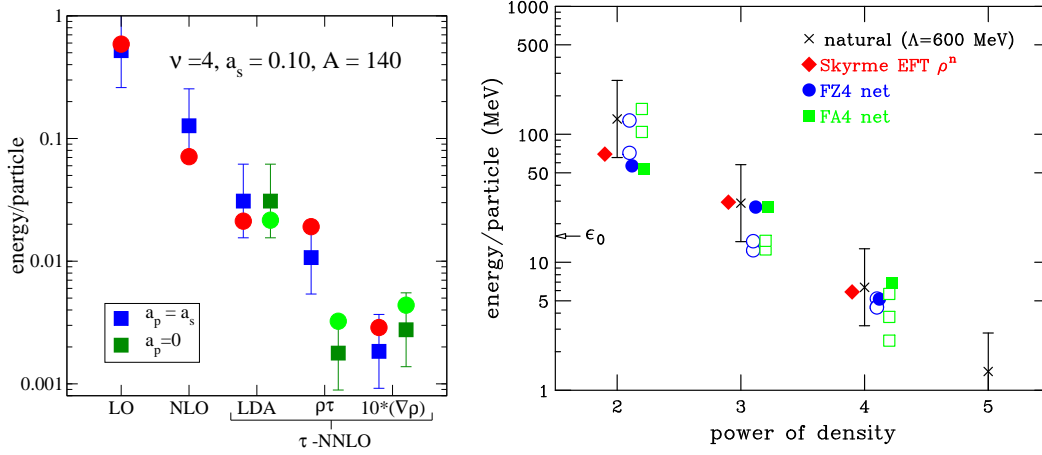


Figure 5: Estimates for energy functionals for a dilute fermions in a harmonic trap (left) and for three phenomenological energy functionals for nuclei (right).

Adding sources coupled to other currents improves the functional variationally and allows pairing to be treated within the same framework [90,91].

Figure 5 shows how EFT power-counting estimates predict the hierarchy of contributions to a DFT energy functional. On the left are results for the energy per particle of  $A = 140$  fermions in a trap with short-range repulsive interactions. The *a priori* estimates from terms at three different orders in the EFT expansion (the counterparts to the terms in Eq. (2) plus gradient corrections) are shown with error bars that reflect a natural range for the unknown coefficients (in this case from  $1/2$  to  $2$ ). These are compared to actual values, with good agreement [90]. A similar exercise using a chiral-EFT-inspired power counting has been applied to phenomenological nonrelativistic (Skyrme) and covariant density functionals. Results for terms organized by powers of the density in each term are shown on the right in Fig. 5 and show that the predicted hierarchy is realized [92,88].

The apparent success of many-body perturbation theory for nuclear matter using low-momentum potentials RG-evolved from chiral EFT input makes feasible the construction of a nuclear DFT functional in the effective action formalism that is compatible with nonrelativistic Skyrme energy functional technology [93,94]. Work is underway as part of a large-scale five-year project to develop a universal nuclear energy density functional (UNEDF) that will cover the entire table of nuclides [95]. The goal is to generate systematically improved energy functionals based on chiral EFT/RG input potentials, including theoretical error estimates so that extrapolation to the driplines is under control.

The density matrix expansion (DME) of Negele and Vautherin [96,97] has been extended to three-body force contributions and applied in momentum space to provide the first-generation functional [88,98]. This construction is facilitated by analytic expressions for the long-range pion contributions derived by Kaiser et al. [78,79]. The functional has the form of a generalized Skyrme functional with density-dependent coefficients, including all allowed terms up to two derivatives, which means it can be directly incorporated into existing computer codes. Cutoff dependence can be used as a diagnostic tool for assessing missing elements of the interaction, the many-body approximations, and the performance of the energy functional. Benchmarking against NCSM and

CC calculations for light- and medium-mass nuclei is possible by calculating the energy with an additional external field, *i.e.*, putting the nuclei in theoretically adjustable traps.

## 4 SUMMARY AND OUTLOOK

Effective field theory is a well-established technique with successes in all branches of physics. Applications of EFT to finite density systems have many precursors stretching back decades but implementations are relatively recent. Many-body systems with short-range interactions are an ideal testing ground for many-body EFT because of the universal nature of the systems and the connection to experiment through cold atom physics.

Far less developed is the application of EFT methods to nuclear many-body systems. The immediate impact of EFT on nuclear many-body calculations is through the systematic organization of effective Hamiltonians for low-energy QCD using chiral effective field theory. Of particular importance is the role of many-body forces. We emphasize that while these Hamiltonians have many successes describing scattering and properties of light nuclei, they are largely untested at densities relevant for most nuclei and nuclear matter. Fortunately, computational tools such as the NCSM, CC, and lattice methods, renormalization group techniques, and density functional theory will funnel advances in chiral EFT to new predictions, so that true tests are forthcoming. More direct applications of EFT methods to many-body calculations are in their infancy but there are clear incentives to pursue them.

This has necessarily been a shallow survey but the breadth of activity should be clear. Key developments are expected in the next few years. These include improvements to the chiral EFT potentials such as full  $N^3\text{LO}$  three-body interactions and the corresponding  $N^3\text{LO}$  Hamiltonian with  $\Delta$  degrees of freedom and the subsequent testing of power counting in light to medium mass systems. In addition, the consistent evolution of many-body forces with RG methods will open the door to the full range of nuclei and nuclear matter.

Beyond the calculational tools, effective field theory provides a new *perspective* for nuclear many-body calculations. Whereas before one sought a universal Hamiltonian for all problem and energy length scales, EFT exploits the infinite number of low-energy potentials: rather than finding the “best” potential we use a convenient or efficient one or work directly from a Lagrangian. For a long time it was hoped that two-body data would be sufficient for nuclear systems; many-body forces were treated as a last resort, to be considered as an add-on. In EFT it is inevitable that many-body forces and data are needed and they are directly tied to the two-body interaction. Before we would avoid divergences and hide them in form factors; with EFT we confront and exploit them (*e.g.*, using cutoff dependence as a tool). Finally, instead of choosing diagrams to sum by “art,” power counting determines what to sum and establishes theoretical truncation errors.

Many relevant and interesting topics were not considered here because of space limitations. Two major (related) areas largely unaddressed are the response to external probes and nuclear reactions. Another area is EFT at high temperature for many-body systems with large scattering length, which has been formulated using the virial expansion [99,100] (see Refs. [101,102] for recent applications of the virial expansion to hot dilute nuclear matter). The EFT formulation of the finite temperature nuclear many-body system with long-range pion interaction is a frontier. Other nuclear systems where EFT can play a particular role are hypernuclei [56] and halo nuclei [103]. Work to apply

EFT methods to covariant hadronic field theories strives to understand the successes of relativistic mean-field phenomenology [104]. Finally, there is the challenge of making the connection to lattice QCD [105] (as opposed to EFT on the lattice).

## Acknowledgments

This work was supported in part by the National Science Foundation under Grant Nos. PHY-0354916 and PHY-0653312, the Department of Energy under Grant No. DE-FG02-03ER4126, and the UNEDF SciDAC Collaboration under DOE Grant DE-FC02-07ER41457.

## LITERATURE CITED

1. National Research Council, *Nuclear Physics: the Core of Matter, the Fuel of Stars* (National Academy Press, Washington, DC, 1999).
2. C. P. Burgess, *Ann. Rev. Nucl. Part. Sci.* **57**, 329 (2007), hep-th/0701053.
3. V. Bernard and U.-G. Meißner, *Ann. Rev. Nucl. Part. Sci.* **57**, 33 (2007), hep-ph/0611231.
4. P. F. Bedaque and U. van Kolck, *Ann. Rev. Nucl. Part. Sci.* **52**, 339 (2002), nucl-th/0203055.
5. S. R. Beane, P. F. Bedaque, W. C. Haxton, D. R. Phillips, and M. J. Savage, nucl-th/0008064.
6. E. Epelbaum, *Prog. Part. Nucl. Phys.* **57**, 654 (2006), nucl-th/0509032.
7. A. L. Fetter and J. D. Walecka, *Quantum Many-Particle Systems* (McGraw-Hill, New York, 1972).
8. H. W. Hammer and R. J. Furnstahl, *Nucl. Phys. A* **678**, 277 (2000), nucl-th/0004043.
9. J. W. Negele and H. Orland, *Quantum Many-Particle Systems* (Addison-Wesley, Redwood City, CA, 1988).
10. E. Braaten and A. Nieto, *Phys. Rev. B* **56**, 14745 (1997).
11. D. Pines, *The Theory of Quantum Liquids* (Addison-Wesley, Menlo Park, 1966).
12. G. Baym and C. Pethick, *Landau Fermi Liquid Theory* (Wiley, New York, 1991).
13. A. A. Abrikosov, L. P. Gorkov, and I. E. Dzyaloshinski, *Methods of Quantum Field Theory in Statistical Physics* (Prentice-Hall, Englewood Cliffs, NJ, 1963).
14. R. Shankar, *Rev. Mod. Phys.* **66**, 129 (1994).
15. J. Polchinski, hep-th/9210046.
16. T. Papenbrock and G. F. Bertsch, *Phys. Rev. C* **59**, 2052 (1999), nucl-th/9811077.
17. M. Marini, F. Pistolesi, and G. C. Strinati, *Eur. Phys. J. B* **1**, 151 (1998).
18. J. Wambach, T. L. Ainsworth, and D. Pines, *Nucl. Phys. A* **555**, 128 (1993).
19. L. P. Gorkov and T. K. Melik-Barkhudarov, *Sov. Phys. JETP* **13**, 1018 (1961).
20. A. Schwenk, B. Friman, and G. E. Brown, *Nucl. Phys. A* **713**, 191 (2003), nucl-th/0207004.
21. D. B. Kaplan, M. J. Savage, and M. B. Wise, *Nucl. Phys. B* **534**, 329 (1998), nucl-th/9802075.
22. C. Regal, *Experimental realization of BCS-BEC crossover physics with a Fermi gas of atoms*, Ph.d thesis, University of Colorado, 2005.
23. R. J. Furnstahl and H. W. Hammer, *Annals Phys.* **302**, 206 (2002), nucl-th/0208058.
24. P. Nikolic and S. Sachdev, *Phys. Rev. A* **75**, 033608 (2007).
25. J. V. Steele, nucl-th/0010066.
26. T. Schäfer, C.-W. Kao, and S. R. Cotanch, *Nucl. Phys. A* **762**, 82 (2005), nucl-th/0504088.



27. G. Rupak, nucl-th/0605074.
28. Z. Nussinov and S. Nussinov, Phys. Rev. A **74**, 053622 (2006), cond-mat/0410597.
29. Y. Nishida and D. T. Son, Phys. Rev. Lett. **97**, 050403 (2006), cond-mat/0604500.
30. P. Arnold, J. E. Drut, and D. T. Son, Phys. Rev. A **75**, 043605 (2007), cond-mat/0608477.
31. S. Weinberg, Phys. Lett. B **251**, 288 (1990).
32. S. Weinberg, Nucl. Phys. B **363**, 3 (1991).
33. C. Ordonez and U. van Kolck, Phys. Lett. B **291**, 459 (1992).
34. S. Weinberg, Phys. Lett. B **295**, 114 (1992), hep-ph/9209257.
35. C. Ordonez, L. Ray, and U. van Kolck, Phys. Rev. Lett. **72**, 1982 (1994).
36. U. van Kolck, Phys. Rev. C **49**, 2932 (1994).
37. C. Ordonez, L. Ray, and U. van Kolck, Phys. Rev. C **53**, 2086 (1996), hep-ph/9511380.
38. S. R. Beane, P. F. Bedaque, M. J. Savage, and U. van Kolck, Nucl. Phys. A **700**, 377 (2002), nucl-th/0104030.
39. A. Nogga, R. G. E. Timmermans, and U. van Kolck, Phys. Rev. C **72**, 054006 (2005), nucl-th/0506005.
40. M. C. Birse, Phys. Rev. C **74**, 014003 (2006), nucl-th/0507077.
41. E. Epelbaum and U. G. Meissner, nucl-th/0609037.
42. D. R. Entem and R. Machleidt, Phys. Rev. C **68**, 041001 (2003), nucl-th/0304018.
43. E. Epelbaum, W. Glockle, and U.-G. Meissner, Nucl. Phys. A **747**, 362 (2005), nucl-th/0405048.
44. E. Epelbaum, Eur. Phys. J. A **34**, 197 (2007), arXiv:0710.4250 [nucl-th].
45. D. Rozpedzik *et al.*, Acta Phys. Polon. B **37**, 2889 (2006), nucl-th/0606017.
46. G. P. Lepage, hep-ph/0506330.
47. G. P. Lepage, nucl-th/9706029.
48. H. Krebs, E. Epelbaum, and U.-G. Meissner, Eur. Phys. J. A **32**, 127 (2007), nucl-th/0703087.
49. E. Epelbaum, H. Krebs, and U.-G. Meißner, arXiv:0712.1969 [nucl-th].
50. S. C. Pieper, Nucl. Phys. A **751**, 516 (2005), nucl-th/0410115.
51. S. C. Pieper, arXiv:0711.1500 [nucl-th].
52. A. Nogga, P. Navratil, B. R. Barrett, and J. P. Vary, Phys. Rev. C **73**, 064002 (2006), nucl-th/0511082.
53. G. Hagen, D. J. Dean, M. Hjorth-Jensen, T. Papenbrock, and A. Schwenk, Phys. Rev. C **76**, 044305 (2007), arXiv:0707.1516 [nucl-th].
54. P. Navratil, V. G. Gueorguiev, J. P. Vary, W. E. Ormand, and A. Nogga, Phys. Rev. Lett. **99**, 042501 (2007), nucl-th/0701038.
55. I. Stetcu, B. R. Barrett, P. Navratil, and J. P. Vary, Phys. Rev. C **73**, 037307 (2006), nucl-th/0601076.
56. A. Nogga, nucl-th/0611081.
57. S. K. Bogner, T. T. S. Kuo, and A. Schwenk, Phys. Rept. **386**, 1 (2003), nucl-th/0305035.
58. S. K. Bogner, R. J. Furnstahl, and R. J. Perry, Phys. Rev. C **75**, 061001 (2007), nucl-th/0611045.
59. R. Roth, H. Hergert, P. Papakonstantinou, T. Neff, and H. Feldmeier, Phys. Rev. C **72**, 034002 (2005), nucl-th/0505080.
60. S. K. Bogner *et al.*, arXiv:0708.3754 [nucl-th].

61. A. Nogga, S. K. Bogner, and A. Schwenk, Phys. Rev. C **70**, 061002 (2004), nucl-th/0405016.
62. G. Hagen *et al.*, Phys. Rev. C **76**, 034302 (2007), arXiv:0704.2854 [nucl-th].
63. R. Roth and P. Navratil, Phys. Rev. Lett. **99**, 092501 (2007), arXiv:0705.4069 [nucl-th].
64. I. Stetcu, B. R. Barrett, and U. van Kolck, Phys. Lett. B **653**, 358 (2007), nucl-th/0609023.
65. W. C. Haxton, arXiv:0710.0289 [nucl-th].
66. R. Brockmann and J. Frank, Phys. Rev. Lett. **68**, 1830 (1992).
67. H. M. Muller, S. E. Koonin, R. Seki, and U. van Kolck, Phys. Rev. C **61**, 044320 (2000), nucl-th/9910038.
68. D. Lee and T. Schäfer, Phys. Rev. C **72**, 024006 (2005), nucl-th/0412002.
69. D. Lee and T. Schäfer, Phys. Rev. C **73**, 015202 (2006), nucl-th/0509018.
70. R. Seki and U. van Kolck, Phys. Rev. C **73**, 044006 (2006), nucl-th/0509094.
71. B. Borasoy, E. Epelbaum, H. Krebs, D. Lee, and U.-G. Meißner, arXiv:0712.2990 [nucl-th].
72. J.-W. Chen and D. B. Kaplan, Phys. Rev. Lett. **92**, 257002 (2004), hep-lat/0308016.
73. S. R. Beane, P. F. Bedaque, A. Parreno, and M. J. Savage, Phys. Lett. B **585**, 106 (2004), hep-lat/0312004.
74. B. Borasoy, E. Epelbaum, H. Krebs, D. Lee, and U.-G. Meissner, Eur. Phys. J. A **31**, 105 (2007), nucl-th/0611087.
75. S. K. Bogner, R. J. Furnstahl, S. Ramanan, and A. Schwenk, Nucl. Phys. A **773**, 203 (2006), nucl-th/0602060.
76. S. K. Bogner, A. Schwenk, R. J. Furnstahl, and A. Nogga, Nucl. Phys. A **763**, 59 (2005), nucl-th/0504043.
77. N. Kaiser, S. Fritsch, and W. Weise, Nucl. Phys. A **697**, 255 (2002), nucl-th/0105057.
78. N. Kaiser, S. Fritsch, and W. Weise, Nucl. Phys. A **724**, 47 (2003), nucl-th/0212049.
79. S. Fritsch, N. Kaiser, and W. Weise, Nucl. Phys. A **750**, 259 (2005), nucl-th/0406038.
80. M. Lutz, B. Friman, and C. Appel, Phys. Lett. B **474**, 7 (2000), nucl-th/9907078.
81. N. Kaiser, M. Muhlbauer, and W. Weise, Eur. Phys. J. A **31**, 53 (2007), nucl-th/0610060.
82. R. M. Dreizler and E. Gross, *Density Functional Theory* (Springer, Berlin, 1990).
83. N. Argaman and G. Makov, Am. J. Phys. **68**, 69 (2000).
84. C. Fiolhais, F. Nogueira, and M. Marques, editors, *A Primer in Density Functional Theory* (Springer, Berlin, 2003).
85. J. Polonyi and K. Sailer, Phys. Rev. B **66**, 155113 (2002), cond-mat/0108179.
86. R. Fukuda, T. Kotani, Y. Suzuki, and S. Yokojima, Prog. Theor. Phys. **92**, 833 (1994).
87. M. Valiev and G. W. Fernando, Phys. Lett. A **227**, 265 (1997).
88. R. J. Furnstahl, nucl-th/0702040.
89. S. J. Puglia, A. Bhattacharyya, and R. J. Furnstahl, Nucl. Phys. A **723**, 145 (2003), nucl-th/0212071.
90. A. Bhattacharyya and R. J. Furnstahl, Nucl. Phys. A **747**, 268 (2005), nucl-th/0408014.
91. R. J. Furnstahl, H. W. Hammer, and S. J. Puglia, Annals Phys. **322**, 2703 (2007), nucl-th/0612086.
92. R. J. Furnstahl, J. Phys. G **31**, S1357 (2005), nucl-th/0412093.
93. J. Dobaczewski, W. Nazarewicz, and P. G. Reinhard, Nucl. Phys. A **693**, 361 (2001), nucl-th/0103001.
94. M. Bender, P.-H. Heenen, and P.-G. Reinhard, Rev. Mod. Phys. **75**, 121 (2003).

- 95. G. F. Bertsch, D. J. Dean, and W. Nazarewicz, *SciDAC Review* **6**, 42 (2007).
- 96. J. W. Negele and D. Vautherin, *Phys. Rev. C* **5**, 1472 (1972).
- 97. J. W. Negele and D. Vautherin, *Phys. Rev. C* **11**, 1031 (1975).
- 98. S. K. Bogner, R. J. Furnstahl, and L. Platter, in preparation.
- 99. P. F. Bedaque and G. Rupak, *Phys. Rev. B* **67**, 174513 (2003), cond-mat/0206527.
- 100. G. Rupak, *Phys. Rev. Lett.* **98**, 090403 (2007), nucl-th/0604053.
- 101. C. J. Horowitz and A. Schwenk, *Nucl. Phys. A* **776**, 55 (2006), nucl-th/0507033.
- 102. C. J. Horowitz and A. Schwenk, *Phys. Lett. B* **638**, 153 (2006), nucl-th/0507064.
- 103. C. A. Bertulani, H. W. Hammer, and U. Van Kolck, *Nucl. Phys. A* **712**, 37 (2002), nucl-th/0205063.
- 104. R. J. Furnstahl, *Lect. Notes Phys.* **641**, 1 (2004), nucl-th/0307111.
- 105. M. J. Savage, nucl-th/0611038.